

STRAIN ENERGY FUNCTION OF RED BLOOD CELL MEMBRANES

R. SKALAK, A. TOZEREN, R. P. ZARDA, and S. CHIEN

From the Department of Civil Engineering and Engineering Mechanics and the Department of Physiology, Columbia University, New York 10027

ABSTRACT The several widely different values of the elastic modulus of the human red blood cell membrane which have been reported in the literature are incorporated into a single strain energy function consisting of two terms. One term gives the small stresses and low elastic modulus which is observed when the red cell membrane is deformed at constant area. The second term contributes a large isotropic stress dependent on the change of area. The strain energy function is applied to the process of sphering of red blood cells in a hypotonic solution. It is shown that a nearly perfect sphere can result even though the red blood cell membrane is homogeneous in all areas of the cell. Results pertinent to sieving and micropipette experiments are also explored.

INTRODUCTION

The first estimate of the elastic modulus of the red cell membrane was given by Katchalsky et al. (1960) based on sphering experiments in a hypotonic solution. The estimated value of the elastic modulus during the spherical phase of the cell and just before hemolysis is 3.1×10^7 dyn/cm².¹ The general range of this estimate was confirmed by Rand (1964) based on experiments in which red cells were sucked into micropipettes of the order of $2 \mu\text{m}$ in diameter. The range of the elastic moduli derived was 7.3×10^6 to 3.0×10^8 dyn/cm². More recently Hochmuth and Mohandas (1972) have reported experiments in which red blood cells adhering to a glass surface were elongated due to shearing stress applied by the flow of the suspending fluid over the cells. Their estimate of the modulus of elasticity is of the order of 10^4 dyn/cm². Another type of test in which the deformed cells were allowed to recover their natural shape gave a value 7.2×10^6 dyn/cm² (Hoeber and Hochmuth, 1970).

The wide range of the elastic moduli quoted above is all the more striking when the strains involved are considered. The elongation in sphering and pipette experiments which give the higher estimates, is about 8%. In the uniaxial tests giving the lowest modulus, the elongation is 40–60%. These strains indicate that the different moduli cannot be interpreted as a nonlinear stiffening of the membrane with in-

¹ The value given by Katchalsky et al. (1960, p. 166) is 2.4×10^7 dyn/cm², but there is a numerical error in computing the radius r_s of a sphere of volume V_s . The corrected value is 3.1×10^7 dyn/cm².

creasing strain. The logical and usual interpretation is that the membrane structure is such that a change of shape at constant area requires relatively small stresses as compared with the stresses required to increase the area of the membrane. The purpose of the present paper is to incorporate this qualitative idea into a specific form using the notion of strain energy as a convenient starting point.

The general idea that the red cell membrane is easily deformed at constant area but that the change in area is always relatively small is supported by numerous tests and observations, particularly by sieving tests (Chien et al., 1971). Red blood cells suspended in Ringer's solution are forced under pressure through polycarbonate sieves which have cylindrical pores about 13 μm long and diameters which are remarkably uniform. When the diameter of pores is greater than 2.8 μm , say 4.4 μm for example, the pressure required to produce a flow of the suspension through the pores at a velocity of 5 mm/s is of the order of 1 mm Hg; but for smaller pores, say 2.2 μm in diameter, a pressure of 100 mm Hg is required to achieve the same velocity and the red cells are hemolyzed to a large extent. At the critical pore diameter of 2.8 μm it is shown that the normal area of the red cell is just sufficient to cover the normal volume of red cell in the shape of a cylinder equal to the pore diameter capped by two hemispherical ends (Gregersen et al., 1967). These results clearly indicate the strong resistance of the red cell membrane to any change in area.

In the subsequent analysis the red blood cell is assumed to consist of an elastic membrane filled with an incompressible viscous fluid. Further, the bending resistance is neglected. These assumptions are reasonable when a red blood cell undergoes large deformations. A discussion of the validity of these assumptions has been given by Fung (1966, 1969) and by Fung and Tong (1968).

THE STRAIN ENERGY FUNCTION

Consider an element of a plane thin membrane originally dx_1 and dx_2 in length parallel to axes x_1 , x_2 shown by the dotted lines in Fig. 1. If tensions T_1 and T_2 (dyne per centimeter) are applied in the x_1 and x_2 directions, the membrane will extend to new lengths dy_1 and dy_2 . The extension ratios λ_1 and λ_2 are defined as the ratios of final to initial lengths:

$$\lambda_1 = \frac{dy_1}{dx_1}, \quad \lambda_2 = \frac{dy_2}{dx_2}. \quad (1)$$

For large deformations, the Green (material) strain tensor may be used also. Its components are defined by

$$e_{11} = \frac{1}{2}(\lambda_1^2 - 1) \quad e_{22} = \frac{1}{2}(\lambda_2^2 - 1). \quad (2)$$

Fung and Tong (1968, Eq. A 11) have suggested a relation between T_1 , T_2 and λ_1 ,

λ_2 which is of the form

$$T_1 = h\mu e_{11} + h\lambda(e_{11} + e_{22}), \quad (3)$$

$$T_2 = h\mu e_{22} + h\lambda(e_{11} + e_{22}), \quad (4)$$

where h is the final thickness of the membrane, and μ and λ are material properties, analogous to Lamé's constants of a linear elastic solid. The parameters μ and λ in Eq. 3 may be functions of the strain invariants I_1, I_2 which are defined by

$$I_1 = e_{11} + e_{22}, \quad (5)$$

$$I_2 = e_{11}e_{22}. \quad (6)$$

In the case of small strains, the invariant I_1 is equal to the areal strain, i.e., the change of area divided by the initial area. The second terms in Eqs. 3 and 4 then yield an isotropic stress field proportional to the areal strain. (Isotropic is used here to denote a state of stress in which $T_1 = T_2$.) The first terms in Eqs. 3 and 4 give stresses whose mean is zero when the areal strain is zero, again, for small strains.

The above concepts are adapted to a description of the red blood cell membrane by the introduction of alternate forms of the invariants defined as

$$I_1 = 2\bar{I}_1 = 2(e_{11} + e_{22}), \quad (7)$$

$$I_2 = 4\bar{I}_2 + 2\bar{I}_1 = 4e_{11}e_{22} + 2(e_{11} + e_{22}), \quad (8)$$

or in terms of λ_1, λ_2 :

$$I_1 = \lambda_1^2 + \lambda_2^2 - 2 \quad (9)$$

$$I_2 = \lambda_1^2\lambda_2^2 - 1 = \left(\frac{dA}{dA_0}\right)^2 - 1 \quad (10)$$

where dA_0 and dA are the initial and final areas of the element shown in Fig. 1. The purpose of introducing I_2 is to have an invariant which is zero when the areal strain is zero regardless of the magnitudes of the extensions λ_1, λ_2 .

Next, a strain energy function is postulated instead of the direct stress-strain relations 3 and 4. In the finite deformation theory of elasticity, the strain energy density \bar{W} per unit of initial volume is assumed to be a function of the Green strain tensor e_{ij} in the general three-dimensional case (see Green and Adkins [1970]) such that

$$s_{ij} = \frac{\partial \bar{W}}{\partial e_{ij}}, \quad (11)$$

where s_{ij} is the Piola-Kirchoff stress tensor which is a stress referred to initial co-

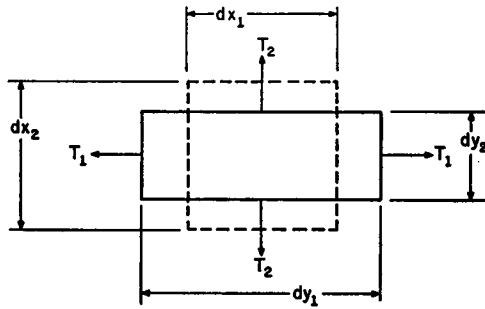


FIGURE 1 Deformation of a membrane element in principal axes. The dotted lines show the original dimensions dx_1 , dx_2 , which are deformed to dy_1 , dy_2 under the action of the tensions T_1 , T_2 .

ordinates. The analogous formulation for the present two-dimensional membrane is

$$S_{ij} = \frac{\partial W}{\partial e_{ij}}, \quad (12)$$

where W is a strain energy per unit of the initial membrane area and S_{ij} is the tension in the membrane (dynes per centimeter) referred to the initial coordinates.

A simple form of the strain energy W which appears to allow description of the red cell membrane properties is

$$W = \frac{B}{4} \left(\frac{1}{2} I_1^2 + I_1 - I_2 \right) + \frac{C}{8} I_2^2, \quad (13)$$

where B and C are membrane material properties which could be functions of I_1 and I_2 in general, but are taken to be constants herein. Substituting Eq. 13 in Eq. 12 and using Eqs. 7 and 8 gives the stress-strain relations

$$S_{11} = Be_{11} + \frac{C}{2} (1 + 2e_{22})I_2, \quad (14)$$

$$S_{22} = Be_{22} + \frac{C}{2} (1 + 2e_{11})I_2. \quad (15)$$

The first terms of Eqs. 14 and 15 are the same form as the first terms of Eqs. 3 and 4. The second terms of Eqs. 14 and 15 give stresses which are zero when the areal strain is zero, whether or not the strains are small. For small strains, Eqs. 14 and 15 may be replaced by the approximations

$$S_{11} = Be_{11} + C(e_{11} + e_{22}), \quad (16)$$

$$S_{22} = Be_{22} + C(e_{11} + e_{22}), \quad (17)$$

which are of the forms 3 and 4.

The Piola-Kirchoff stress tensor s_{ij} is related to the usual spatial or Eulerian stress tensor σ_{ij} in three-dimensional theory of elasticity by (Green and Adkins, 1970)

$$\sigma_{ij} = \frac{1}{J} s_{kl} \frac{\partial y_i}{\partial x_k} \frac{\partial y_j}{\partial x_l}, \quad (18)$$

where y_i is the final coordinate, and x_k is the initial coordinate, and J is the determinant

$$J = \left| \frac{\partial y_i}{\partial x_j} \right|. \quad (19)$$

Similarly in the present two-dimensional theory of membranes, the usual tensions per unit length in the final position T_1, T_2 are related to the Piola-Kirchoff tensions S_1, S_2 by

$$T_{ij} = \frac{1}{J} S_{kl} \frac{\partial y_i}{\partial x_k} \frac{\partial y_j}{\partial x_l}, \quad (20)$$

where y_i is the final coordinate, and x_k is the initial coordinate, and J is the determinant

$$J = \left| \frac{\partial y_i}{\partial x_j} \right| = \lambda_1 \lambda_2. \quad (21)$$

In Eqs. 18 and 19 the range of the indices is 1, 2, 3, but is only 1, 2 in Eqs. 20 and 21. Using Eqs. 1, 14, 15, and 21 in Eq. 20 gives, after some reduction, the final stress-strain relations proposed for the red cell membrane:

$$T_1 = \frac{\lambda_1}{\lambda_2} \left[\frac{B}{2} (\lambda_1^2 - 1) + \frac{C}{2} \lambda_2^2 I_2 \right], \quad (22)$$

$$T_2 = \frac{\lambda_2}{\lambda_1} \left[\frac{B}{2} (\lambda_2^2 - 1) + \frac{C}{2} \lambda_1^2 I_2 \right]. \quad (23)$$

These stress-strain relations are nonlinear when regarded either as functions of the extension ratios λ_1, λ_2 or the Green (material) strains e_{11}, e_{22} . For small strains, the tensions T_1, T_2 become equal to S_{11}, S_{22} and the linear equations, Eqs. 16 and 17, may be used for T_1 and T_2 . The concept of strain energy function may be used to generate descriptions of materials with more severe nonlinearity than Eqs. 22 and 23 by appropriate choice of the strain energy function. For example, the membrane becomes exponentially stiff with increasing areal strain if the strain energy function Eq. 13 is replaced by

$$W = \frac{B}{4} \left(\frac{1}{2} I_1^2 + I_1 - I_2 \right) + C' [\cosh (kI_2) - 1], \quad (24)$$

where B, C' , and k are material properties.

For any choice of a strain energy function $W(I_1, I_2)$ the tensions are:

$$T_1 = 2 \frac{\lambda_1}{\lambda_2} \left(\frac{\partial W}{\partial I_1} + \lambda_2^2 \frac{\partial W}{\partial I_2} \right), \quad (25)$$

$$T_2 = 2 \frac{\lambda_2}{\lambda_1} \left(\frac{\partial W}{\partial I_1} + \lambda_1^2 \frac{\partial W}{\partial I_2} \right). \quad (26)$$

The present state of knowledge of the red cell membrane properties does not seem to warrant a more complex form for W than Eq. 13. The constants in this form may be adjusted to represent existing data approximately by the following procedures.

The constant C is chosen to be much larger than the constant B in Eq. 13 so that the areal stiffness is appropriately large. A representative value of the elastic modulus for areal extension, discussed in the Introduction above is 10^7 dyn/cm². This modulus may be designated as an areal modulus K defined by

$$K = \lim_{e_{11} \rightarrow 0} \frac{T_1}{e_{11} h}, \quad (T_1 = T_2), \quad (27)$$

where it is to be understood that $e_{11} = e_{22}$ and $T_2 = T_1$ as the limit is approached. K is of the nature of a two-dimensional analogue of bulk modulus, observed under isotropic stress, $T_1 = T_2$. The thickness of the membrane h is assumed to be 100 Å when the strains are zero. Then the assumption of $K = 10^7$ dyn/cm² gives a value of $C = 5$ dyn/cm by using Eq. 22 in Eq. 27.

The data on uniaxial stretching of red cells mentioned in the Introduction is taken to have a representative value of 10^4 dyn/cm². This modulus is interpreted to be that observed when a tension T_1 is applied and the membrane is otherwise free so that $T_2 = 0$. This gives Young's modulus E defined by

$$E = \lim_{e_{11} \rightarrow 0} \frac{T_1}{e_{11} h} \quad (T_2 = 0), \quad (28)$$

where it is to be understood that $T_2 = 0$ as the limit is approached. The assumption of $E = 10^4$ dyn/cm² and $h = 100$ Å gives a value of $B = 0.5 \times 10^{-2}$ dyn/cm.

The results of adopting the above values of B and C are illustrated in Fig. 2 and compared with available experimental data for the uniaxial tension test with $T_2 = 0$. It may be seen that the curve developed from Eqs. 22 and 23 lies in about the middle of the range given by Hochmuth and Mohandas (1972). The areal strain, $(dA/dA_0 - 1) = (\lambda_1 \lambda_2 - 1)$, is also shown in Fig. 2. The change of area during the uniaxial tension test is about 0.01% in the proposed material. This is in agreement

with the observation of Hochmuth and Mohandas (1972) that the area appeared to be approximately constant in their tests.

The stress-strain curve for isotropic tension ($T_1 = T_2$) is shown in Fig. 3 for the proposed red cell membrane material. No detailed experimental data are available

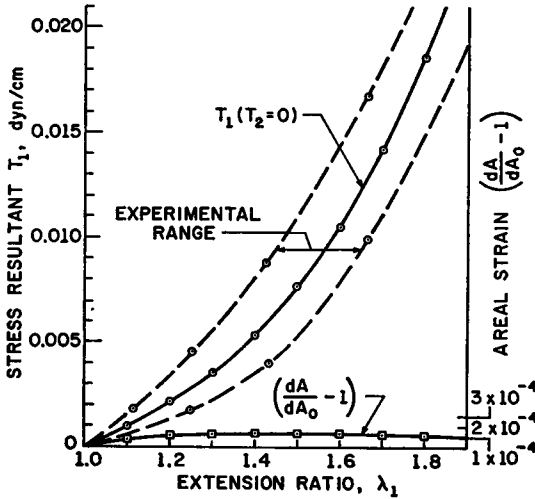


FIGURE 2 Stress-strain curve T_1 vs. λ_1 in uniaxial tension for proposed red cell membrane strain energy function, Eq. 13. The dotted lines show the range suggested by Hochmuth and Mohandas (1972) on the basis of experiments on whole red cells. Note that the areal strain curve is nearly zero (right-hand scale).

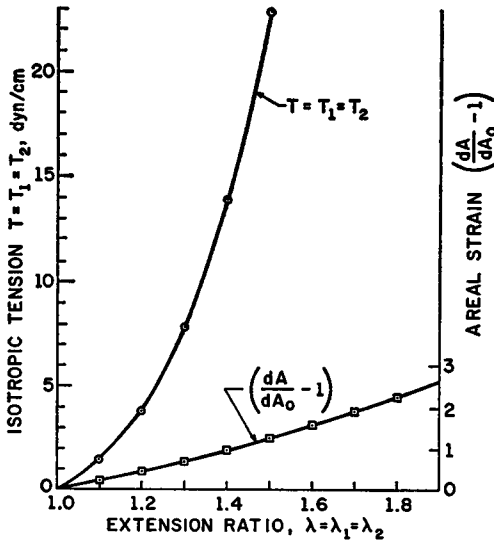


FIGURE 3 Stress-strain curve in isotropic tension for proposed red cell membrane strain energy function, Eq. 13. Note that the tensions and areal strains are much larger than in Fig. 2.

for comparison, but the initial modulus K in Fig. 3 is 10^7 dyn/cm². Note that the tensions in Fig. 3 are about three orders of magnitude greater than in Fig. 2. The areal strain, $(\lambda_1\lambda_2 - 1)$ is also shown in Fig. 3 and is equal to $(\lambda_1^2 - 1)$ in this case. The red cell membrane will rupture, according to Rand (1964), when the elongation $(\lambda_1 - 1)$ in isotropic tension is about 0.08.

It is of interest to compare the behavior of the red cell membrane with that of a rubber sheet of the same thickness because rubber has been used for models of red cells by a number of investigators. Further, rubber is a material that has been studied theoretically and experimentally. Rubber may be regarded as isotropic and incompressible with a strain energy function of the so-called Mooney-Rivlin material (Green and Adkins, 1970):

$$W = C_1(I_1 - 3) + C_2(I_2 - 3), \quad (29)$$

where

$$I_1 = \lambda_1^2 + \lambda_2^2 + \lambda_3^2, \quad (30)$$

$$I_2 = \lambda_1^{-2} + \lambda_2^{-2} + \lambda_3^{-2}. \quad (31)$$

The condition of incompressibility is

$$\lambda_3 = \frac{1}{\lambda_1\lambda_2}, \quad (32)$$

where λ_3 is the extension ratio in the direction perpendicular to the plane of the membrane. The tensions T_1 , T_2 are given by

$$T_1 = \frac{2h_0}{\lambda_1\lambda_2} \left(\lambda_1^2 - \frac{1}{\lambda_1^2\lambda_2^2} \right) (C_1 + \lambda_2^2 C_2), \quad (33)$$

$$T_2 = \frac{2h_0}{\lambda_1\lambda_2} \left(\lambda_2^2 - \frac{1}{\lambda_1^2\lambda_2^2} \right) (C_1 + \lambda_1^2 C_2), \quad (34)$$

where h_0 is the initial thickness of the membrane. The ratio of the two constants, C_2/C_1 is 0.1 according to Green and Adkins (1970, p. 168). The magnitude of C_1 and C_2 may be adjusted to give the Young modulus measured in uniaxial tension for example by Sutura et al. (1970) in their rubber red cell models. This value is $E = 10^7$ dyn/cm² and leads to the values $C_1 = 2.57 \times 10^6$ dyn/cm² and $C_2 = 0.257 \times 10^6$ dyn/cm². These constants give the results shown in Fig. 4 for uniaxial and isotropic tension for a membrane initially 100 Å thick. The most striking difference is that the stresses in uniaxial tension and isotropic tension are of the same order of magnitude for rubber (Fig. 4) but are three orders of magnitude different for the red cell membrane (Figs. 2 and 3). This difference is also reflected in the curves of areal strain. The red cell membrane has very little change of area in uniaxial tension (Fig. 2), but

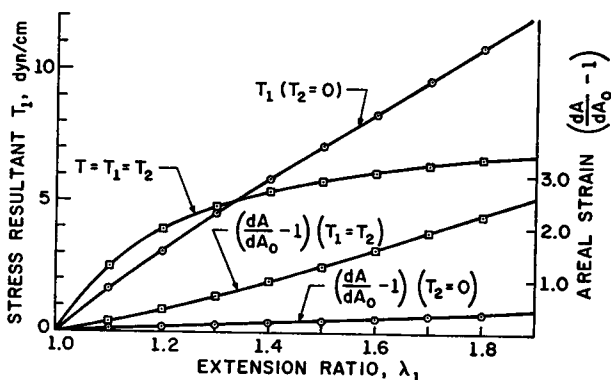


FIGURE 4 Uniaxial tension $T_1(T_2 = 0)$ and isotropic tension ($T_1 = T_2$) stress resultants for a membrane of rubber having the same initial thickness (100 \AA) as a red cell membrane. Note the large areal strain in both cases.

rubber has an areal strain in uniaxial tension given by (Fig. 4)

$$\left(\frac{dA}{dA_0} - 1\right) = (\lambda_1^{1/2} - 1). \quad (35)$$

This is easily derived from the requirement $T_2 = 0$ which is achieved by setting the first bracket in Eq. 34 equal to zero.

The above results suggest that rubber is qualitatively not a good material to represent the red cell membrane. The magnitudes of elastic moduli are not important in modeling, but the relative behavior in uniaxial tension and isotropic tension is important to the qualitative behavior and is not modeled by rubber.

A further comparison of red cell membrane and rubber membrane may be illustrated by constructing contours of the strain energy functions in the plane (λ_1, λ_2) as shown in Figs. 5 and 6. The lines labeled $\lambda_1\lambda_2 = 1$ represent the locus of points of constant area. The lines $\lambda_1 = \lambda_2$ represent isotropic tension. In the case of the red cell membrane, Fig. 5, the strain energy changes slowly along the curve of constant area, and hence produces only small stresses; but any departure from the constant area line produces a sharp rise in strain energy and large stresses. The strain energy of rubber is much more insensitive to changes in area (Fig. 6). This results in a significant difference of behavior of red cell membrane and rubber in that compressive stresses (negative tensions) do not develop as readily in red cell membrane when the area is slightly increased as compared with rubber. Of course, thin membranes buckle readily under any compressive stresses. It may therefore be expected that wrinkling (buckling) of rubber membranes will be more often observed than in red cell membranes.

In Eq. 13, the constants B and C have the units of dynes per centimeter and may be regarded as an elastic modulus (dynes per square centimeter) times a thickness h (centimeters). The expression of the constants in dynes per centimeter obviates

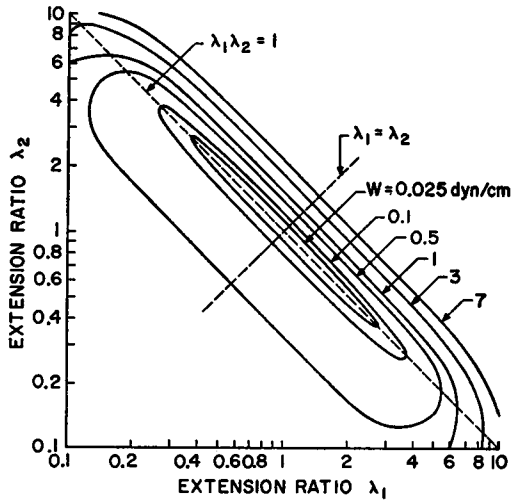


FIGURE 5 Strain energy contours in the plane λ_1, λ_2 for the red cell membrane according to Eq. 13. Note log-log scale in which the line $\lambda_1\lambda_2 = 1$ represents constant area and the line $\lambda_1 = \lambda_2$ represents isotropic tension.

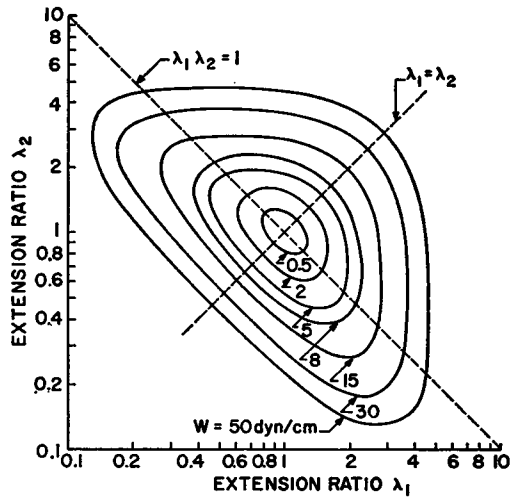


FIGURE 6 Strain energy contours in the plane λ_1, λ_2 for a rubber sheet having the thickness of a red cell membrane. The strain energy is given by Eq. 29 for rubber.

the need to know the thickness and hence eliminates one troublesome (and unnecessary) unknown in dealing with experimental data. A modulus (dynes per square centimeter) can be recouped by dividing B or C by an assumed or measured thickness h .

The direct approach of treating the tensions (dynes per centimeter) and the extension ratios λ_1, λ_2 or Green's strains e_1, e_2 as primary quantities in a two-

dimensional theory is more completely developed in the Appendix. It is also of interest to show that the forms suggested above, e.g. Eqs. 13, 24, 25, and 26, can be regarded as the consequence of a particular case of three-dimensional theory of anisotropic finite deformation elasticity. A convenient starting point is the strain energy of a transversely isotropic material given by Green and Adkins (1970, p. 26). The directions 1, 2 are isotropic, and the transverse direction, 3, is different. Then the strain energy W is

$$W = W(I_1, I_2, I_3, K_1), \tag{36}$$

where the invariants are:

$$I_1 = 3 + 2(e_{11} + e_{22} + e_{33}), \tag{37}$$

$$I_2 = 3 + 4(e_{11} + e_{22} + e_{33}) + 4(e_{11}e_{22} + e_{11}e_{33} + e_{22}e_{33}), \tag{38}$$

$$I_3 = (1 + 2e_{11})(1 + 2e_{22})(1 + 2e_{33}), \tag{39}$$

$$K_1 = e_{33}^2 \tag{40}$$

Now if we restrict to an incompressible material, I_3 equals 1 and drops out of consideration. Next, assume that I_1 , I_2 , and K_1 enter only in the following combinations:

$$I_1 - 2K_1 - 3 = I_1, \tag{41}$$

$$I_2 - 3 - 4K_1 - (I_1 - 2K_1 - 3)(1 + 2K_1) = I_2; \tag{42}$$

The invariants I_1 and I_2 in Eqs. 41 and 42 are the same as in Eqs. 9 and 10. By assuming that W depends on the combinations of I_1 , I_2 , and K_1 given in Eqs. 41 and 42, the general expressions for the tensions in a transversely isotropic membrane reduce to the previous forms 25 and 26. This shows that Eqs. 22 and 26 and hence Eq. 13 define a possible subclass of transversely isotropic materials. The above manipulation brings out one further fact, namely, the kind of membrane represented by Eq. 13 or Eqs. 22 and 23 is one in which the strains in the transverse (x_3) direction have no influence on the stresses T_1 and T_2 . This is reasonable for the red cell membrane.

All of the above discussion, starting with Fig. 1 and Eq. 1, tacitly assumes that the coordinate axes x_1 , x_2 are the directions of the principal axes of strain. Such axes always exist, but in axes which are not principal there may be a shear stress resultant T_{12} in the plane of the membrane. Expressions for T_{12} are given in the Appendix.

Some limiting cases of the red cell membrane strain energy function proposed in Eq. 13 are of interest as possible simplified models for the red cell membrane in approximate computations.

(a) The case in which C is finite but B is equal to zero gives a membrane in which T_1 is always equal to T_2 and has a magnitude depending on the change in area which may vary from point to point.

(b) The case of C approaching infinity with B finite gives a membrane which cannot be forced to increase its area, but it has a finite modulus in uniaxial tension. In uniaxial tension, or any other state of stress, its area is constant. The tensions T_1 and T_2 are indeterminate to the extent of an isotropic tension which may vary with position.

(c) The case of C approaching infinity and B equal to zero gives a membrane of constant area. The tensions T_1 and T_2 are equal at any point, but may vary with position.

Probably a is a reasonable approximation in late stages of sphering. It is essentially the assumption made by Katchalsky et al. (1960), Rand and Burton (1964), and Rand (1964).

The cases b and c may be useful in approximating the behavior of red cells in flow through capillaries, in sieving tests, and shear flows in general. These possibilities are discussed further below.

APPLICATIONS

For illustrative purposes, the red blood cell is assumed to have the unstressed shape shown in Fig. 7. This shape is adapted from Fung and Tong (1968). Restricting to cases in which the deformed shape of the red blood cell is also axisymmetric, the principal axes of stress and strain are the meridional and circumferential directions, so Eqs. 22 and 23 are sufficient to describe the elastic behavior of the membrane. The equations of equilibrium of the membrane under a normal stress or pressure p across the membrane are (Flügge, 1964):

$$\frac{\partial}{\partial s} (RT_1) - r_1 T_2 \cos \phi = 0, \quad (43)$$

$$\frac{T_1}{r_1} + \frac{T_2}{r_2} = p, \quad (44)$$

where r_1 and r_2 are the principal radii of curvature in the deformed position, R is the cylindrical radius, and ϕ is the angle (n, z) as indicated in Fig. 7. The tension T_1 acts in the meridional direction and T_2 is the circumferential or hoop stress. The distance s is measured along the deformed membrane surface along a meridian.

Consider the sphering of a red blood cell in a hypotonic solution in the extreme case c above, i.e., $B = 0$, $C \rightarrow \infty$. Suppose that the volume of the cell adjusts itself by transfer of fluid through the membrane until the internal pressure of the cell is a certain amount p above the pressure in the external fluid. The value of p is controlled by the osmolarity of the suspending fluid. In the extreme case c , there always exists a solution for the deformed shape of the cell which is a perfect sphere that

(a)

$$Z^2 = (0.86)^2(1-X^2)(C_0 + C_1 X^2 + C_2 X^4)$$

$$-1 \leq X \leq 1$$

$C_0 = 0.01384083$
 $C_1 = 0.2842917$
 $C_2 = 0.01306932$
 $Z^1 = 4.2Z; X^1 = 4.2X$

VOLUME $91.52 \mu\text{m}^3$
 SURFACE AREA $141.61 \mu\text{m}^2$
 SPHERICITY INDEX 0.694

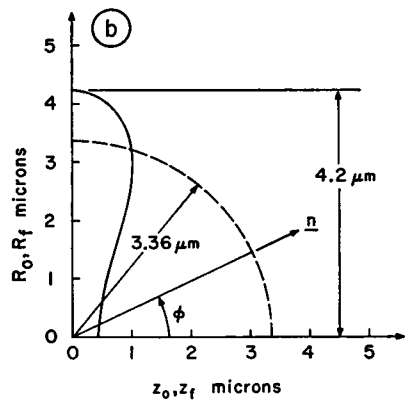
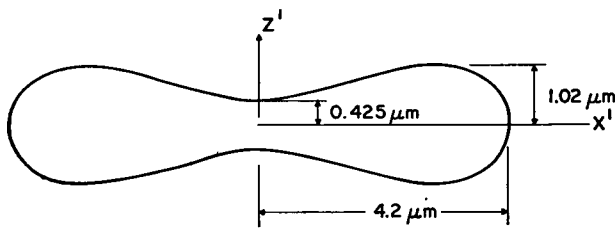


FIGURE 7 (a) Unstressed shape of the red blood cell membrane assumed for illustrative purposes. Adapted from Fung and Tong (1968). (b) Spherized red cell (dotted curve) having the same surface area as the assumed unstressed shape shown in a. Initial coordinates R_0, z_0 . Final coordinates are R_f, z_f or ϕ, r .

has the same total area as the original shape. For the red blood cell shown in Fig. 7 a, the initial area is $141.6 \mu\text{m}^2$ and the sphere which has the same area has a radius of $3.36 \mu\text{m}$. This sphere is shown as the dashed circle in Fig. 7 b. The present theory requires that not only the total area of the original red cell and the sphere be equal, but also that areal strain at every point of the sphere be zero. The resultant distribution of extension ratios λ_1 (in the meridonal direction) and λ_2 (circumferential) are shown in Fig. 8. The values of λ_1 and λ_2 are computed from the assumed shapes in Fig. 7, and the requirement $\lambda_1\lambda_2 = 1$ for zero areal strain. In Fig. 8, λ_1 and λ_2 are plotted against angular position ϕ on the final sphere; $\phi = 0$ indicates points initially on the axis of the red blood cell. The computation proceeds easily from $\phi = 0$ where it is required that $\lambda_1 = \lambda_2 = 1$ for constant area. It is remarkable that λ_1 and λ_2 remain nearly equal to unity up to $\phi \approx 30^\circ$ in Fig. 8. This is due to the

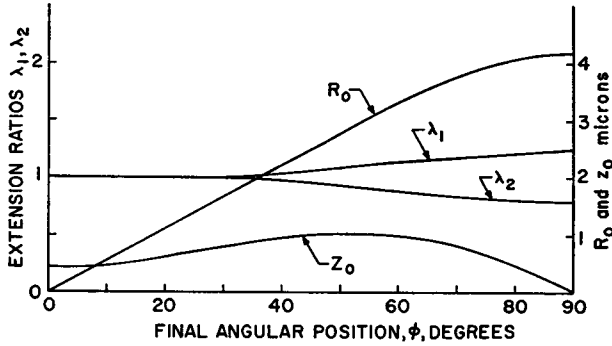


FIGURE 8 Extension ratios λ_1 (in the meridonal direction) and λ_2 (circumferential) for the case of a red cell sphering without change of area as shown in Fig. 7. The initial coordinates R_0 , z_0 are also shown as a function of final angular position, ϕ . These curves completely specify the deformation.

fact that the initial red cell shape in Fig. 7 has very nearly the same curvature near the axis as the final spherical shape.

Whenever B equals zero, the two principal tensions T_1 and T_2 are equal at each point. If $C \rightarrow \infty$, any value of the isotropic tension can be achieved with essentially zero change in area. In the limit $C \rightarrow \infty$, the stress distribution in the sphere in Fig. 7 is the value required by Eq. 44:

$$T = T_1 = T_2 = rp/2, \tag{45}$$

where r is the radius of the sphere. Here $r = r_0 = 3.36 \mu\text{m}$.

Next, consider the case of sphering a red blood cell with $B = 0$ and $C = C_0 =$ finite constant. For any internal pressure p above the external pressure, there is again a solution which is a sphere because $B = 0$. For an infinitesimal pressure difference p , the radius of the sphere is $r = r_0 = 3.36 \mu\text{m}$, but as p increases, the radius increases. The pressure is given in terms of r by

$$p = \frac{C}{r_0} \frac{r}{r_0} \left[\left(\frac{r}{r_0} \right)^4 - 1 \right]. \tag{46}$$

The above two cases are unrealistic in that every value of $p > 0$ yields a perfect sphere for the deformed shape. This is because $B = 0$. If $B > 0$, then a spherical shape will be approached gradually. The actual process of sphering of a red blood cell is recorded in the photographs presented by Canham and Parkinson (1970). The shape of the cell changes gradually but always has very nearly the same surface area. In the early stages of sphering, bending stresses which have been neglected herein may also play a significant role.

To estimate the degree of departure from a perfect sphere that may be expected in a red cell membrane with the constants developed above ($B = 0.005 \text{ dyn/cm}$,

$C = 5 \text{ dyn/cm}$) consider that at sufficiently high pressure, the sphere shown in Fig. 7 and the strains shown in Fig. 8 are a good approximation at some pressure p , say $p = 5,000 \text{ dyn/cm}^2$. This is about half of the typical pressure estimated by Katchalsky et al. (1960) to produce hemolysis. The tension computed by Eq. 45 for this pressure is $T = 0.840 \text{ dyn/cm}$. This is to be compared with the stresses associated with the coefficient B in Eq. 13 and the strains in Fig. 8. For the values of λ_1 and λ_2 in Fig. 8, an upper bound for the stresses T_1 and T_2 is 0.00221 dyn/cm . Since these stresses are only about 0.3 % of the isotropic stress, it may be expected that a perturbation of the spherical shape of the order of 0.3 % of the radius will give an equilibrium position when these stresses are taken into account. (Detailed computations of all stages of sphering of red blood cells are underway to support these estimates and will be reported in a subsequent paper.)

Another simple example of some interest is shown in Fig. 9. A plane circular membrane of radius b is mounted over a rigid circular plate which has a hole of radius $R = a$ cut out of its center. The membrane and plate are fastened to a rigid cylinder at radius $R = b$ (Fig. 9 A). In Figs. 9 B, 9 C, and 9 D, the membrane (only) is shown inflated by a pressure p applied to the upper face of the membrane. In each case, a solution exists in which the inflated portion of the membrane is part of a spherical surface. It is assumed here that the constants in Eq. 13 are B equals zero and C equals a constant. In this case, $T_1 = T_2 = T$ at each point and in this example the tension T is a constant throughout the membrane. At the edge of the supporting plate at $R = a$, the membrane is supposed to slide freely so that the

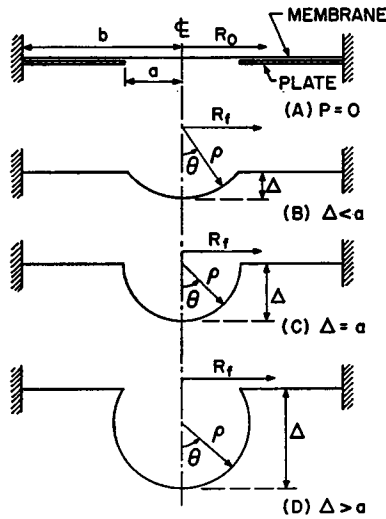


FIGURE 9. Deformation of a plane circular membrane of radius b , mounted over a plate with a circular hole of radius a . The unstressed initial position is shown in A. The inflation under increasing pressure is illustrated in B, C, and D. In each case, the entire membrane undergoes uniform isotropic tension and uniform areal strain α .

tensions are continuous at this point. Between $R = a$ and $R = b$, the membrane is also assumed to slide freely although the pressure p presses the membrane against the plate.

The solution is easily expressed by assuming the spherical radius ρ of the inflated portion of the membrane is given. Then the areal ratio $\alpha = A/A_0$ for the entire membrane is

$$\alpha = \frac{A}{A_0} = \frac{b^2 - a^2}{b^2} + \frac{2\rho^2}{b^2} \left[1 \pm \left(1 - \frac{a^2}{\rho^2} \right)^{1/2} \right], \quad (47)$$

where A and A_0 are the final and initial areas of the membranes; in Eq. 47 the minus sign applies to Fig. 9 B where the maximum deflection Δ is less than a ; the plus sign applies to Fig. 9 D where $\Delta > a$. In any case, the uniform tension is

$$T = \frac{C}{2} \alpha(\alpha^2 - 1), \quad (48)$$

and the applied pressure p is

$$p = \frac{C}{\rho} \alpha(\alpha^2 - 1). \quad (49)$$

The points on the deflected portion of the membrane can be located by the angle θ (Figs. 9 B, C, and D) which is given in terms of the initial radius R_0 (Fig. 9 A) by

$$\cos \theta = 1 - \frac{1}{2\rho^2} \alpha R_0^2. \quad (50)$$

The portion of the membrane with a final position radius R_f lying over the plate is related to its initial position by

$$R_f = [\alpha(R_0^2 - b^2) + b^2]^{1/2}, \quad a \leq R_f \leq b. \quad (51)$$

The above solution may have bearing on experiments in which a portion of a red cell membrane is sucked into a pipette (Rand and Burton, 1964; Weed and Lacelle, 1969) and on sieving experiments (Chien et al., 1971). In analyzing these experiments, these authors assume the deflected portion of the membrane is part of a spherical surface. The above example suggests this is possible when B equals zero and C equals a constant. For the red cell membrane, B is much smaller than C and hence very nearly spherical surfaces should be expected.

In the above solutions there is an increase of the area of the membrane, but the same series of spherical caps (Figs. 9 B, C, and D) could be achieved without areal strain in the case $B = 0$, $C = \infty$ if the membrane was allowed to move inwards (radially) from the support at $R = b$ (Fig. 9 A). Such a case probably corresponds more closely to sieving and pipette experiments.

DISCUSSION

The proposed strain energy function given by Eq. 13 appears to be adequate to represent the elastic behavior of the red blood cell membrane in a variety of situations including uniaxial tension, sphering, sieving tests, and micropipette tests. It is therefore of interest to speculate on the detailed structure of the red blood cell membrane that could result in this kind of elasticity.

The materials comprising the red blood cell membrane can probably be regarded as incompressible in a three-dimensional sense, i.e., the volume of material is constant. In deformations in which the area of the membrane remains constant, the incompressibility in a three-dimensional sense results in the thickness of the membrane being constant during the deformation. When the area of the membrane is increased, as in sphering experiments just before hemolysis, the membrane thickness may or may not remain constant. If no holes open up, the thickness must decrease as the area increases. There is also the possibility that the thickness of the membrane remains constant and that the increased area is provided by the creation of minute holes in the membrane. The two-dimensional formulation leading to Eq. 13 does not distinguish between the two possibilities. It is possible that the progressive enlargement of minute holes with increasing areal strain is the structural basis of hemolytic loss of cell contents and ultimate rupture. It is pertinent that nearly circular holes with diameters of 80–100 Å have been demonstrated in erythrocyte membrane after immune hemolysis (Borsos et al., 1964). In osmotic hemolysis (Hjelm et al., 1966) and mechanical hemolysis (Chien et al., 1971), membrane holes of similar dimensions have also been inferred from the relative quantities of release of different sizes of molecules from the red cells.

Electron microscope studies on red cell membrane have provided some ultrastructural information on membrane structure. Examining the red cell ghost membranes by electron microscopy and metal shadowing, Hillier and Hoffman (1953) have reported that the membrane consists of short cylinders (or plaques) with heights of approximately 30 Å and diameters of 100–500 Å. Cylindrical particles approximately 100 Å in diameter and normal to cell surface have been demonstrated in the membrane interior by the use of a freeze-cleaving technique (Branton, 1966; Weinstein and McNutt, 1970). A model of the red cell membrane composed of cylindrical apoprotein molecules bound at their central belts by lipids has been suggested by Zahler (1969).

A fluid mosaic model of the structure of cell membranes in general, including the red cell membrane, has been developed by Singer and Nicolson (1972). Most of the area of the typical membrane is a lipid bilayer with polar head groups of the lipids on both faces of the membrane and fatty acid chains extending inward from the faces. This matrix is regarded as a two-dimensional liquid. Protein molecules are embedded in the lipid matrix and may extend completely through the membrane to form a two-dimensional fluid mosaic. In any case, the thickness of the red blood

cell membrane up to the point of rupture is either constant or varies at most by about 15% while the elongations in a given direction tangential to the membrane can be 100% or more. This behavior suggests that there should be expected some comparatively stiff structures in the transverse direction of the membrane which preserve the thickness. The lipid molecule matrix could perform this function. The fluidity of the mosaic may account for the small resistance of the red cell membrane to changes in shape. The stiffness of the membrane to any change in area represented by the coefficient C in Eq. 13 could be provided if the lipid molecules were relatively free to move about, but had strong attractive and repulsive forces, like the molecules of a liquid, which kept their average spacing constant. The mechanical behavior of the red blood cell membrane proposed above is thus consistent with the fluid mosaic model of the structure of the membrane.

In summary, the red cell membrane behaves like a two-dimensional version of a soft, but nearly incompressible material. It is a two-dimensional analogue of the three-dimensional behavior of a substance like rubber which is nearly incompressible but easily deformed. If rubber is cast into a thin sheet, however, it preserves its volume but not its area when stressed. The red cell membrane tends to preserve its area, but otherwise deforms readily.

This research was supported by National Institutes of Health, National Heart and Lung Institute through grant no. 2R01-HL 13083-03-CVB, U. S. Army Medical Research and Development Command Contract DADA-17-72-C-2115 and the Scaife Family Charitable Trust, Pittsburgh, Pa.

Received for publication 5 June 1972.

REFERENCES

- BORSOS, T., R. R. DOURMASHKIN, and J. H. HUMPHREY. 1964. *Nature (Lond.)* 202:251.
- BRANTON, D. 1966. *Proc. Natl. Acad. Sci. U.S.A.* 55:1048.
- CANHAM, P. B., and D. R. PARKINSON. 1970. *Can. J. Physiol. Pharmacol.* 48:369.
- CHIEN, S., S. A. LUSE, and C. A. BRYANT. 1971. *Microvasc. Res.* 3:183.
- FLÜGGE, W. 1964. Springer-Verlag, Berlin.
- FUNG, Y. C. 1966. *Fed. Proc.* 25:1761.
- FUNG, Y. C. 1969. *J. Biomech.* 2:353.
- FUNG, Y. C., and P. TONG. 1968. *Biophys. J.* 8:175.
- GREEN, A. E., and J. E. ADKINS. 1970. Large Elastic Deformations. The Oxford University Press, London. 2nd edition.
- GREGERSEN, M. I., C. A. BRYANT, W. E. HAMMERLE, S. USAMI, and S. CHIEN. 1967. *Science (Wash. D. C.)* 157:825.
- HILLIER, J., and J. F. HOFFMAN. 1953. *J. Cell. Comp. Physiol.* 42:203.
- HJELM, M., S. G. OSTLING, and A. E. G. PERSSON. 1966. *Acta Physiol. Scand.* 67:43.
- HOCHMUTH, R. M., and N. MOHANDAS. 1972. *J. Biomech.* 5:501.
- HOEBER, T. W., and R. M. HOCHMUTH. 1970. Transactions of the American Society of Mechanical Engineers, Series D. *J. Basic Eng.* 92:604.
- KATCHALSKY, A., O. KEDEM, C. KLIBANSKY, and A. DeVRIES. 1960. In Flow Properties of Blood and Other Biological Systems. A. L. Copley and G. Stainsby, editors. Pergamon Press, New York. 155.
- RAND, R. P. 1964. *Biophys. J.* 4:303.
- RAND, R. P., and A. C. BURTON. 1964. *Biophys. J.* 4:115.
- SINGER, S. J., and G. L. NICOLSON. 1972. *Science (Wash. D. C.)* 175:720.

SUTERA, S. P., V. SESHADRI, P. A. CROCE, and R. M. HOCHMUTH. 1970. *Microvasc. Res.* 2:420.
 WEED, R. I., and P. L. LACELLE. 1969. *In Red Cell Membrane: Structure and Function*. G. A. Jamieson and T. J. Greenwalt, editors. J. B. Lippincott Company, New York. 318-338.
 WEINSTEIN, R. S., and N. S. MCNUTT. 1970. *Semin. Hematol.* 7:259.
 ZAHLER, P. 1969. *Experientia (Basel)*. 25:449.

APPENDIX

Membrane Stresses in Nonprincipal Axes

In the body of the paper, starting with Fig. 1 and Eq. 1, it was tacitly assumed that the directions of the principal axes of stress and strain were known and parallel to x_1, x_2 . The membrane stresses and invariants were given in terms of principal strains for brevity. These expressions are sufficient if the principal directions are known. The general deformation of a plane membrane in its own plane is considered below.

Let the deformations of a plane membrane be described by initial and final positions in cartesian coordinates x_1, x_2 and y_1, y_2 , respectively. The Green (material) strain tensor is defined by

$$e_{ij} = \frac{1}{2} \left(\frac{\partial y_k}{\partial x_i} \frac{\partial y_k}{\partial x_j} - \delta_{ij} \right), \quad (\text{A } 1)$$

where the range of all indices is 1, 2 and the usual summation convention holds for repeated indices. The invariants I_1 and I_2 defined by Eqs. 7 and 8 are

$$I_1 = 2 \operatorname{tr}[e_{ij}] = 2(e_{11} + e_{22}), \quad (\text{A } 2)$$

$$I_2 = 2 \operatorname{tr}[e_{ij}] + 4 \det[e_{ij}] = 2(e_{11} + e_{22}) + 4[e_{11}e_{22} - e_{12}^2], \quad (\text{A } 3)$$

where tr and \det stand for trace and determinant.

Using Eqs. A 2 and A 3 in the strain energy $W(I_1, I_2)$, the Piola-Kirchoff stresses Eq. 12 are

$$S_{11} = 2 \frac{\partial W}{\partial I_1} + (2 + 4e_{22}) \frac{\partial W}{\partial I_2}, \quad (\text{A } 4)$$

$$S_{12} = S_{21} = -4e_{12} \frac{\partial W}{\partial I_2}, \quad (\text{A } 5)$$

$$S_{22} = 2 \frac{\partial W}{\partial I_1} + (2 + 4e_{11}) \frac{\partial W}{\partial I_2}. \quad (\text{A } 6)$$

The membrane stresses T_{ij} in the final (spatial) coordinates are given by Eq. 20 which are in full

$$T_{11} = \frac{1}{J} \frac{\partial y_1}{\partial x_i} \frac{\partial y_1}{\partial x_j} S_{ij}, \quad (\text{A } 7)$$

$$T_{12} = T_{21} = \frac{1}{J} \frac{\partial y_1}{\partial x_i} \frac{\partial y_2}{\partial x_j} S_{ij}, \quad (\text{A } 8)$$

$$T_{22} = \frac{1}{J} \frac{\partial y_2}{\partial x_i} \frac{\partial y_2}{\partial x_j} S_{ij}, \quad (\text{A } 9)$$

where

$$J = \det \left[\frac{\partial y_i}{\partial x_j} \right], \quad (\text{A } 10)$$

and the repeated indices indicate summation over 1, 2. The stresses T_{12} and T_{21} are shearing forces per unit length which act parallel to the edge of the membrane element. In principal axes, Eqs. A 7 and A 8 reduce to Eqs. 25 and 26 and the shears T_{12} and T_{21} are zero.